Simple sol-gel combustion synthesis and characterizations studies of spinel Sm-$ZnFe_2O_4$ ferrite nano-particles

Govindaswamy Padmapriya [a], Pandian Paulraj [b]

[a, b]Department of Chemistry, Faculty of Arts & Science, Bharath Univerisity, selaiyur, Chennai-73, Tamilnadu, India

Abstract

Spinel $Sm_xZn_{1-x}Fe_2O_4$ (x = 0.0 and 0.3) nanoparticles were synthesized by combustion method. The samples were characterized by XRD, HR-SEM and VSM analysis. The powder XRD confirms that all the compositions crystallize with cubic spinel $ZnFe_2O_4$ and $SmFe_2O_4$. HR-SEM images revealed that the samples are crystalline with particle size distribution in 20-22 nm range. The saturation magnetization (M_s) increased with increase in Sm content.

Keywords: Microwave combustion; Spinel ferrites; Electron microscopy; Magnetic properties.

*** : Corresponding author: E-mail:** ppstminex@gmail.com (Dr. G. Padmapriya)

1. Introduction

Nanocrystalline spinel ferrites possess unique structural and opto-magnetic properties than that of their same bulk counterparts [1-3]. Spinel ferrites have applications in the area of magnetic resonance imaging and multilayer chip indicator, etc. Spinel ferrites with a general

formula MFe_2O_4 (M= Co^{2+}, Sm^{3+}, Zn^{2+}, etc.) have been investigated for their usual optical and magnetic properties. Zinc ferrite ($ZnFe_2O_4$) is a normal spinel structure with Zn^{2+} ions located at the tetrahedral sites and Fe^{3+} ions at the octahedral sites [4-6]. $ZnFe_2O_4$ is a commercially important material and has been widely used in many areas, such as photo-catalysts, gas sensors, catalysts, absorbent materials and information storage [7,8].

Spinel Ni-$ZnFe_2O_4$ ferrite has attracted a vast of interest, because of its high resistivity, high permeability, and low dielectric loss in high frequency device applications. Many methods have been used to prepare the spinel ferrite nanoparticles, such as solvothermal, co-precipitation, hydrothermal, sol–gel [9-11]. Nevertheless, the above methods have some disadvantages such as, high-energy consuming, requirement of complicated equipment, requirement of a strong base, like NaOH, higher processing temperature and also require rather long reaction time to complete the crystallization of $ZnFe_2O_4$ [12].

Microwave combustion method has recently gained importance than the above said methods. The microwaves interact with the reactants at the molecular level, which leads to a uniform heating. During the microwave combustion, the microwave energy is transferred and converted into heat, because of the motion of the molecules. This results in the formation of $ZnFe_2O_4$ nanoparticles within few minutes of time and leads to a higher efficiency [13].

In this present study, we have synthesized $Sm_xZn_{1-x}Fe_2O_4$ (x = 0.0 and 0.5) nanoparticles by microwave combustion method using glycine as the fuel. The structural phase of the prepared samples was characterized by powder X-ray diffraction (XRD) analysis. The particle size and morphologies were determined by high resolution scanning electron microscopy (HR-SEM) and the chemical composition was determined by the energy dispersive X-ray (EDX) analysis. The magnetic behavior of the samples was studied by the vibrating sample magnetometer (VSM).

2. Experimental

2.1. Materials and methods

All the chemicals used in this study were of analytical grade obtained from Merck, India and were used as received without further purification. $Zn(NO_3)_2 \cdot 6H_2O$, 98%, $Fe(NO_3)_3 \cdot 9H_2O$, 98% and $Sm(NO_3)_2$ were used as precursors and $C_2H_5NO_2$ as a fuel for this method.

2.2. Characterization techniques

The structural characterization of spinel $Sm_xZn_{1-x}Fe_2O_4$ (x = 0.0 and 0.5) nanoparticles were performed using a Rigaku Ultima X-ray diffractometer equipped with Cu-Kα radiation (λ = 1.5418 Å). Morphological studies and energy dispersive X-ray analysis of Sm-doped $ZnFe_2O_4$ nanoparticles have been performed with a Jeol JSM6360 high resolution scanning electron microscope (HR-SEM). Magnetic measurements were carried out at room temperature using a PMC MicroMag 3900 model vibrating sample magnetometer (VSM) equipped with 1 T magnet.

3. Results and discussion

3.1. XRD analysis

The structural analysis of $Sm_xZn_{1-x}Fe_2O_4$ (x = 0.0 and 0.3) samples was done by powder X-ray diffraction (XRD) technique using Cu Kα radiation. Fig. 1a,b shows the XRD patterns of $Sm_xZn_{1-x}Fe_2O_4$ (x = 0.0 and 0.3) samples. There is no additional peak for all compositions, which indicates that all the samples crystallize in single-phase cubic structure with Fd3m space group [14].

In addition, the crystallite size is estimated from the most intense (311) reflection peak using the Debye Scherrer formula,

$$L = \frac{0.89\lambda}{\beta \cos\theta}$$

where L is the crystallite size, λ , the X-ray wavelength, θ, the Bragg diffraction angle and β, the full width at half maximum (FWHM). The crystallite size of $ZnFe_2O_4$ and $Sm_{0.5}Zn_{0.5}Fe_2O_4$ samples are 26.21, and 25.13 nm, respectively. It shows clearly that by increasing the amount of Sm^{2+} ions, the crystallite size decreased. It is observed that lattice parameter decreased from 8.443 Å to 8.436 Å with increase in nickel concentration, which attributes to the replacement of larger Zn^{2+} (0.83 Å) ions by smaller Sm^{2+} (0.79 Å) ions [15].

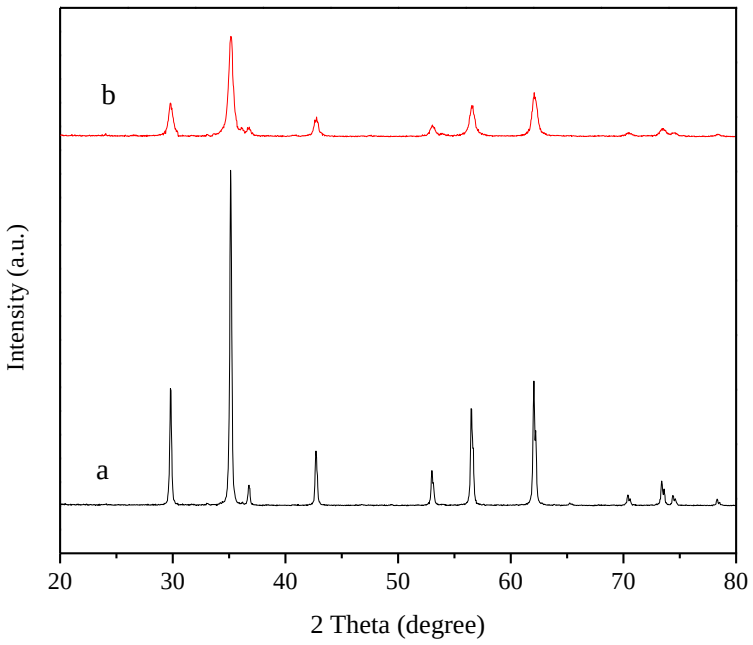

Figure 1. XRD patterns of (a) $ZnFe_2O_4$ and (b) $Sm_{0.3}Zn_{0.7}Fe_2O_4$.

3.2. Scanning electron microscopy (SEM) studies

High resolution scanning electron microscope (HR-SEM) studies was used to investigate the microstructures with the change in Ni composition in $ZnFe_2O_4$ nanoparticles. HR-SEM micrographs of the as-synthesized samples exhibited uniform, almost spherical shaped and loosely agglomerated particles as shown in Fig. 2 a,b. The average particle size of the ferrite nanoparticles prepared via this route is found to be in the range of 20-22 nm. It is observed that the particle size increases as the concentration of Ni ion increases.

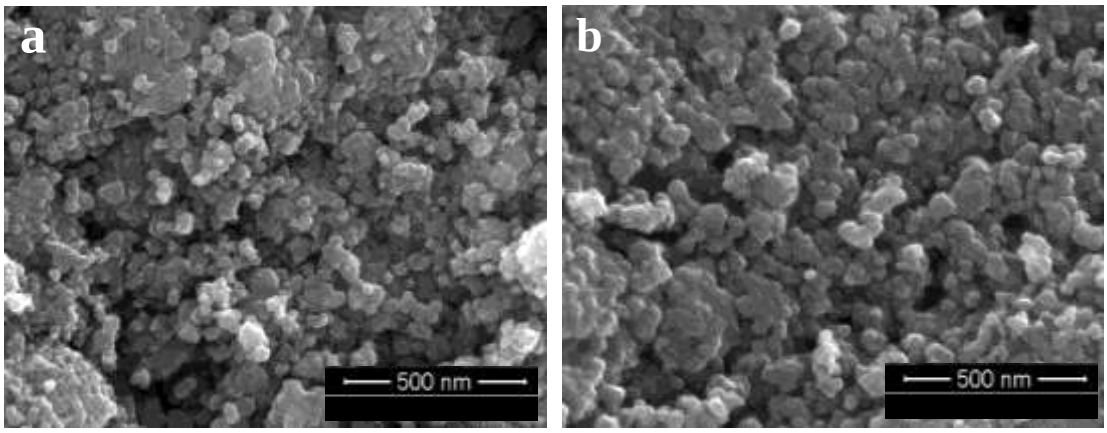

Figure 2. HR-SEM images of (a) $ZnFe_2O_4$ and (b) $Sm_{0.3}Zn_{0.7}Fe_2O_4$.

3.3. Energy dispersive X-ray analysis (EDX)

Energy dispersive X-ray analysis (EDX) of the respective samples is shown in Fig. 3. The peaks corresponding to the elements Fe, Zn and O were observed in pure $ZnFe_2O_4$ (Fig. 3) and the peaks of the elements Fe, Zn, Sm and O were observed in Sm-doped $ZnFe_2O_4$ samples (Fig. 3).

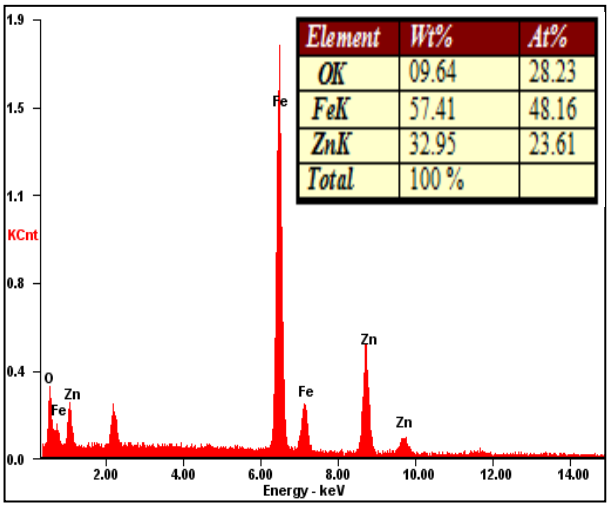

Figure 3. EDX spectra of $ZnFe_2O_4$

3.4. Magnetic measurements (VSM)

The magnetic property of the as-prepared $ZnFe_2O_4$ and $Sm_{0.3}Zn_{0.7}Fe_2O_4$ nanoparticles was investigated with a vibrating sample magnetometer (VSM). Fig. 4 shows the magnetic measurements of $ZnFe_2O_4$ and $Sm_{0.3}Zn_{0.7}Fe_2O_4$ samples. From the VSM measurements saturation magnetization (M_s), remanent magnetization (M_r) and coercivity (H_c) values are evaluated. From the results, it is clearly understood that the magnetic properties of the samples are affected by the composition and cation distribution [16]. The magnetization curve demonstrates a typical superparamagnetic behavior of the as-prepared pure $ZnFe_2O_4$ nanoparticles with lower remanence and coercivity. This is confirmed by the non saturation

observed in MH loop and the absence of the hysteresis, M_r and H_c. The superparamagnetic nature can be attributed to their fine crystalline size, which makes it easier for them to be thermally activated to overcome the magnetic anisotropy [17]. For $Sm_{0.3}Zn_{0.7}Fe_2O_4$ sample, a hysteresis was observed, thus indicating the ferromagnetism. This is due to the increase in the magnetic nature of the Sm^{2+} concentration.

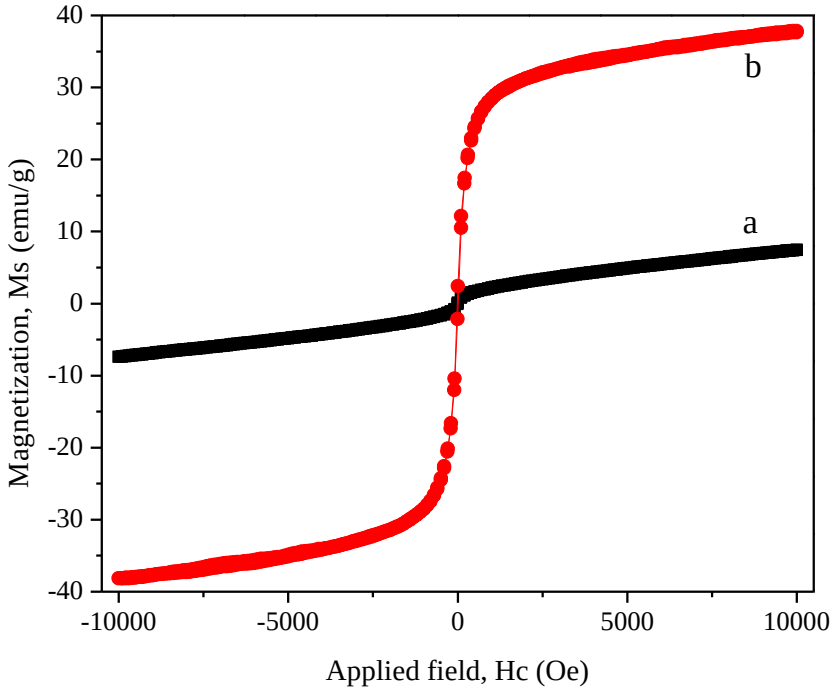

Figure 4. Magnetic hysteresis loops of (a) $ZnFe_2O_4$ and (b) $Sm_{0.3}Zn_{0.7}Fe_2O_4$

4. Conclusions

Nanocrystalline $Sm_xZn_{1-x}Fe_2O_4$ (x = 0.0 and 0.3) nanoparticles were successfully prepared by microwave combustion method using glycine as the fuel. Microwave combustion method is suitable for preparing the spinel structure with good crystallinity and reproducibility.

The crystallite size was found to vary within the range of 25.21 to 26.13 nm. The results revealed that the decreases in Zn concentration lead to the decrease in particle size, which ultimately affects the magnetic properties of the sample.

References

1. M. Zheng, X. C. Wu, B. S. Zou, Y. J. Wang, Magnetic properties of nanosized $MnFe_2O_4$ particles, J. Magn. Magn. Mater. 183 (1998) 152-156.
2. O. T. B. Ulrich, I. T. Michael, G. Kaul, M. S. Nikolic, B. Mollwitz, R. A. Sperling, R. Reimer, H. Hohenberg, W. J. Parak, S. F.G. Adam, H. Weller, N. C. Bigall, Size and surface effects on the MRI relaxivity of manganese ferrite nanoparticle contrast agents, Nano Lett. 7 (2007) 2422-2427.
3. B. D. Cullity, Introduction to Magnetic Materials, Addison-Wesley, New York, 1972.
4. T. Sato, K. Haneda, M. Seki, T. Iijima, Morphology and magnetic properties of ultrafine $ZnFe_2O_4$ particles, Appl. Phys. A 50 (1990) 13-16.
5. C. N. Chinnasamy, A. Narayanasamy, N. Ponpandian, K. Chattopadhyay, H. Guerault, J. M. Greneche, Magnetic properties of nanostructured ferrimagnetic zinc ferrite, J. Phys. Condens. Matter 12 (2000) 7795-7805.
6. A. Manikandan, L. John Kennedy, M. Bououdina, J. Judith Vijaya, Synthesis, optical and magnetic properties of pure and Co-doped $ZnFe_2O_4$ nanoparticles by microwave combustion method, Journal of Magnetism and Magnetic Materials, 349 (2014) 249-258.
7. D. K. Manimegalai, A. Manikandan, S. Moortheswaran, S. Arul Antony, Magneto-Optical and Photocatalytic Properties of Magnetically Recyclable $Zn_{1-x}Mn_xS$ (x = 0.0, 0.3

and 0.5) nano-catalysts, Journal of Superconductivity and Novel Magnetism, 28, 9, (2015) 2755-2766.

8. A. Manikandan, R. Sridhar, S. Arul Antony, S. Ramakrishna, A simple aloe vera plant-extracted microwave and conventional combustion synthesis: Morphological, optical and catalytic properties of magnetic $CoFe_2O_4$ nanostructures, Journal of Molecular Structure, 1076 (2014) 188-200.
9. A. Manikandan, M. Durka, S. Arul Antony, A novel synthesis, structural, morphological and opto-magnetic characterizations of magnetically separable spinel $Co_xMn_{1-x}Fe_2O_4$ ($0 \leq x \leq 1$) nano-catalysts, Journal of Superconductivity and Novel Magnetism, 27 (2014) 2841–2857.
10. V. Umapathy, A. Manikandan, S. Arul Antony, P. Ramu, P. Neeraja, Synthesis, structural, morphological and opto-magnetic properties of Bi_2MoO_6 nano-photocatalyst by sol-gel method, Transactions of Nonferrous Metals Society of China, 25 (2015) 3271-3278.
11. J. Li, Z. Huang, D. Wu, G. Yin, X. Liao, J. Gu, D. Han, Preparation and protein detection of Zn-Ferrite film with magnetic and photoluminescence properties, J. Phys. Chem. C 114 (2010) 1586-1592.
12. P. H. Borse, J. S. Jang, S. J. Hongand J. S. Lee, J. H. Jung, T. E. Hong, C. W. Ahn, E. D. Jeong, K. S. Hong, J. H. Yoon, H. G. Kim, Photocatalytic hydrogen generation from water-methanol mixtures using nanocrystalline $ZnFe_2O_4$ under visible light irradiation, J. Korean Phys. Soc. 55 (2009) 1472-1477.

13. A. Van Dijken, E.A. Meulenkamp, D. Vanmaekelbergh, A. Meijerink, Identification of the transition responsible for the visible emission in ZnO using quantum size effects, J. Lumin. 90 (2000) 123-128.
14. S. Ayyappan, S. Philip Raja, C. Venkateswaran, J. Philip, B. Raj, Room Temperature Ferromagnetism in vacuum annealed $ZnFe_2O_4$ nanoparticles, Appl. Phys. Lett. 96 (2010) 143106.
15. G.F. Goya, H.R. Rechenberg, Ionic disorder and Neel temperature in $ZnFe_2O_4$ nanoparticles, J. Magn. Magn. Mater. 196-197 (1999) 191-192.
16. T. Yamanaka, M. Okita, Magnetic properties of the Fe_2SiO_4-Fe_3O_4 spinel solid solutions, Phys. Chem. Miner. 28 (2001) 102-109
17. M. Bohra, S. Prasad, N. Kumar, D.S. Misra, S. C. Sahoo, N. Venkataramani, R. Krishnan, Large room temperature magnetization in nanocrystalline zinc ferrite thin films, Appl. Phys. Lett. 88 (2006) 262506.